



Therapeutic Potential of *Oxalis latifolia*: Phytochemical Profiling and Green Synthesis of Functional Nanoparticles

Malavika J , Athira P , Gayathri G , Slowmo M , Thenmozhi Krishnasamy

[The author informations are in the declarations section. This article is published by ETFLIN in Sciences of Phytochemistry, Volume 5, Issue 1, 2026, Page 122-134. DOI: 10.58920/sciphy0501522]

Received: 03 December 2025

Revised: 12 February 2026

Accepted: 03 March 2026

Published: 06 May 2026

Editor: Khafit Wiradimafan



This article is licensed under a Creative Commons Attribution 4.0 International License. © The author(s) (2025).

Keywords: Phytomedicine, Pharmacology, Medicinal plants, Phytoconstituents, In vitro, AgNPs.

Abstract: This study comprehensively evaluated the phytochemical profile, antioxidant potential, and nanobiotechnological applications of *Oxalis latifolia*. Extractive yields varied significantly ($p < 0.05$), with ethanolic extracts of the stem and leaf providing the highest yields at 20.65% and 13.83%, respectively. Quantitative analysis revealed that ethanolic extracts were particularly rich in bioactive compounds, with the stem showing the highest total phenolic content (79.32 mg GAE/g) and total tannins (69.33 mg GAE/g), while the leaf contained 62.50 mg RE/g of flavonoids. These high concentrations correlated with potent antioxidant activity; the ethanolic leaf extract exhibited a DPPH scavenging IC_{50} of 92.18 $\mu\text{g/mL}$, which was compared against the Ascorbic Acid positive control ($IC_{50} = 26.63 \mu\text{g/mL}$). Furthermore, silver nanoparticles (AgNPs) were successfully biosynthesized using the leaf extract, characterized by a distinct surface plasmon resonance peak at 405 nm and an average size of 56.68 nm. The synthesized AgNPs demonstrated significant dose-dependent anti-inflammatory efficacy, achieving a maximum protein denaturation inhibition of 82.35% at 100 $\mu\text{g/mL}$ ($R^2 = 0.9993$), compared to the Diclofenac Sodium control which reached 95.12%. These findings highlight the potential of *O. latifolia* as a sustainable source for functional nanomaterials.

Introduction

Since ancient times, medicinal plants have been witnessed for their curative properties and employed by many different civilizations all over the world as a valuable source of natural medical care. The importance of medicinal plants has not waned as humanity has advanced into the modern period; scientific studies continue to demonstrate how these plants contribute to human health and their well-being. New chemical discoveries have been made possible by the abundance of natural products. The significance of therapeutic plants goes beyond their ability to treat illness. They are very much essential for the normal functioning of global healthcare systems, particularly in areas where access to traditional medicine is either severely restricted or unaffordable. Additionally, the sustainable use of medicinal plants encourages socio-economic growth and biodiversity conservation, especially in rural areas that totally depend on traditional herbal medicinal practices (1). A critical awareness of the chemical makeup of medicinal plants and a methodical screening process are prerequisites to investigating their potential

medicinal value and ultimately result in the identification of a novel drug source (2).

Secondary metabolites produced by plants have been classified into many classes, such as phenols, flavonoids, alkaloids, tannins, glycosides, coumarins, etc., depending on their chemical structures. The majority of these phytochemical substances function as strong starting points for the synthesis of drugs that are either used as single agents or, through their synergistic action, may engage several target sites to fight illnesses (3). In general, plants have garnered significant interest in managing disorders associated with oxidative stress due to their broad ethnopharmacological functions and in treating diseases. Antioxidants combat chronic illnesses like cancer, diabetes, cardiovascular diseases, etc. and also neutralise the body's production of free radicals (4).

The family Oxalidaceae possesses an extensive spectrum of phytochemical components, notably phenolic acids, alkaloids, and flavonoids, each of which are bioactive compounds that contribute to its curative properties. These chemical compounds have an array of pharmacological properties, such as antibacterial, anti-inflammatory, antioxidant, and anticancer properties. For

instance, oxalic acid, which is abundant in the *Oxalis* species, is well-known for possessing antioxidant properties (5).

Oxalis latifolia, a member of the family Oxalidaceae, is often referred to as 'garden pink sorrel' or 'broadleaf woodsorrel'. This perennial herb emerges from a small bulb and spreads through stolons, lacking a distinct stem. Its leaves are borne on lengthy ground-level petioles, which consist of three broadly heart-shaped leaflets, each measuring approximately 4.5 cm wide (6). The *Oxalis* genus is extensively utilised in traditional medicine for various ailments such as ulcers, wound healing, dysentery, diarrhoea, quartan fever, skin issues, wart removal, corneal cloudiness, and vomiting in children (7). This genus is known for its antibacterial, anti-inflammatory and antiscorbutic properties (8). However, limited research exists on the species *O. latifolia*, particularly from an integrated perspective that connects its phytochemical composition with nanobiotechnological applications. Since phenolic compounds, flavonoids, and other secondary metabolites are known to function as natural reducing and stabilising agents in the green synthesis of metallic nanoparticles, systemic phytochemical profiling is essential to understand their role in nanoparticle formation and their bioactivity. Therefore, the present study is focused mainly on the phytochemical profiling, *in vitro* antioxidant capabilities of the *O. latifolia* crude extracts, the characterisation and *in vitro* anti-inflammatory efficacy of the silver nanoparticles derived from the plant extract to determine their biological performance.

Methodology

Collection and Authentication of the Plant

Fresh plant specimens were collected from The Nilgiris, Western Ghats. The plant samples were duly identified and authenticated by Dr V. Aravindhan, Assistant Professor, Department of Botany, Kongunadu Arts and Science College, Coimbatore.

Preparation of the Plant Sample

Fresh leaves and stem parts were washed, shade-dried at room temperature and finely powdered using a Hammer Mill pulverizer.

Preparation of Crude Plant Extracts

The air-dried powdered plant samples (15 g/150 mL) were successively extracted in increasing order of polarity using petroleum ether, ethyl acetate, and ethanol for about 48 h, while aqueous extraction was carried out using the cold maceration technique for 48 h under controlled laboratory conditions. All extractions were performed in triplicate to ensure reproducibility and consistency, and the extracts were then concentrated to dryness. The extractive yield percentage for the respective solvents was calculated and stored for further detailed studies (9).

Proximate Composition Analysis

The proximate compositional analysis for crude lipids, total carbohydrates, and total proteins was performed to provide a comprehensive biochemical baseline profile of

the plant material using established standard analytical procedures (10).

Preliminary Phytochemical Screening

The preliminary qualitative phytochemical analysis of leaves of *O. latifolia* was carried out using standard qualitative colour-based assays to identify the primary and secondary metabolites using standard procedures as an initial assessment (11).

Quantification of Secondary Metabolites From Different Solvent Extracts

Estimation of Total Phenol Content

Total phenolic content was measured using the Folin-Ciocalteu method. Standard solutions and 1mg of plant extract were dissolved in 1 mL of distilled water, then mixed with Folin-Ciocalteu reagent and sodium carbonate. After incubation, absorbance at 725 nm was recorded and phenolic content was reported as milligrams of gallic acid equivalents (12).

Estimation of Total Tannin Content

Total tannin content was measured using the Folin-Ciocalteu method. Tannins were separated by PVPP precipitation and centrifuged to obtain free phenolics. Gallic acid standards and 100 μ L of test samples were mixed with Folin-Ciocalteu reagent and sodium carbonate, and then incubated in the dark. Absorbance at 725 nm was measured to determine the total phenolics (12). Total tannin content was then calculated as follows Eq. 1.

Estimation of Total Flavonoid Content

Total flavanol content was determined using the Aluminium chloride method. Standard and sample solutions were mixed with aluminium chloride and sodium acetate, then incubated at 20 °C for 2.5 h, and absorbance at 440 nm was measured. Flavanol content was expressed as mg rutin equivalents/g sample (14). For all spectrophotometric estimations, calibration curves were constructed using appropriate standard compounds (gallic acid for phenolics and tannins; rutin for flavonoids and flavanols) at different concentrations within the linearity range. The regression equations and correlation coefficients (R^2) were determined to ensure linearity of response. All measurements were performed in triplicate, and results were expressed as mean \pm standard deviation. These rigorous statistical measures were implemented to ensure the reproducibility of the data and the precision of the phytochemical quantification.

Estimation of Total Flavanol Content

Total flavanol content was determined using the Aluminium chloride method. Standard and sample solutions were mixed with aluminium chloride and sodium acetate, then incubated at 20 °C for 2.5 h, and absorbance at 440 nm was measured. Flavanol content was expressed as mg rutin equivalents/g sample (14). For all spectrophotometric estimations, calibration curves were constructed using appropriate standard compounds (gallic acid for phenolics and tannins; rutin for flavonoids and

$$\text{Total Tannins (g)} = \text{Total Phenols (g)} - \text{Total Free Phenols (g)} \quad (\text{Eq. 1})$$

flavanols) at different concentrations within the linearity range. The regression equations and correlation coefficients (R^2) were determined to ensure linearity of response. All measurements were performed in triplicate, and results were expressed as mean \pm standard deviation.

In vitro Antioxidant Activity

DPPH Scavenging Activity

The DPPH scavenging activity of *O. latifolia* was determined according to the method described (15). Different concentrations of the extract in methanol were mixed with 5 mL of 0.1 mM DPPH and incubated for 20 min at 27 °C. Absorbance at 517 nm was measured in the dark. Ascorbic acid was used as a positive control, while methanol with DPPH was used as the reagent blank. The percentage of inhibition is based on DPPH colour reduction. All experiments were performed in triplicate. The percentage of inhibition from the absorbance of the sample was measured using the following Eq. 2:

The IC₅₀ (Inhibitory Concentration 50 %) from the concentration and percentage inhibition graph was calculated.

ABTS^{•+} Scavenging Activity

The ABTS^{•+} scavenging activity of the plant extract was measured according to the method described (16). Trolox was used as the reference standard, and ethanol with ABTS^{•+} solution served as the negative control. 1 mL of diluted ABTS solution was added to various sample concentrations and Trolox standards in ethanol, and the absorbance at 734 nm was measured 30 min after mixing. Total antioxidant activity (TAA) was expressed as μ M Trolox equivalents per gram of extract from the standard curve. All measurements were carried out in triplicate.

Phosphomolybdenum Assay

The Phosphomolybdenum assay of *O. latifolia* was carried out according to the method described (17). 1 mL of reagent was added to various sample concentrations. The mixture was incubated at 95 °C for 90 min, cooled, and the absorbance at 765 nm was measured. Ascorbic acid was used as the positive control, while reagent solution with extract served as blank. Results were expressed as ascorbic acid equivalents per gram of extract (AEAC). All assays were performed in triplicate.

Synthesis of Silver Nanoparticles (AgNPs)

Green synthesis of silver nanoparticles (AgNPs) was achieved using *O. latifolia* whole plant extract. Using a bottom-up approach with slight modifications from the previous literature (18). Plant extract was prepared at a concentration of 5 mg/mL and filtered before use. 250 mL solution of 0.1 mM silver nitrate was pre-cooled at 0 °C for 2 h and then added dropwise into 250 mL of *O. latifolia* extract under magnetic stirring. The reduction of Ag⁺ ions

into Ag⁰ was observed at room temperature (30 °C), indicated by a colour change from light yellow to dark yellow and finally to colloidal brown after overnight incubation. The reaction kinetics of AgNPs were monitored using a UV-Visible spectrometer (UV-1800, Shimadzu, Japan) at regular time intervals of 30 min until stabilisation of the surface plasmon reference peak. After overnight incubation, the reaction mixture was centrifuged at 10,000 rpm for 30 min and washed three times with distilled water to remove unbound biomolecules and the resulting pellets were collected for further analysis. The nanoparticle yield was calculated based on the dry weight of the obtained pellet relative to the initial silver nitrate used. All syntheses were performed in triplicate to assess batch-to-batch consistency.

UV-Vis Spectroscopy

The optical properties of the synthesised silver nanoparticles (AgNPs) were monitored using a UV-Vis spectrometer (19). A Thermo Scientific Evolution 201 instrument equipped with 10-mm quartz cuvettes was used for recording the absorbance spectra. Spectra were collected in the wavelength range of 200–800 nm to detect the characteristic surface plasmon resonance (SPR). The characteristic surface plasmon resonance (SPR) peak, usually appearing between 400–450 nm and thus the analysis records a SPR peak at 405 nm on the sample.

Scanning Electron Microscope (SEM) Analysis

The element analysis of the silver nanoparticles was performed using EDX on the SEM. The freeze-dried silver nanoparticles were mounted on specimen stubs with double-sided tape, coated with gold in a sputter coater (BAL-TEC SCD-005), and examined under a TESCAN-MIRA3 XMU SEM at 15 kV. Scanning electron microscopy provided further insight into the morphology and size details of the silver nanoparticles.

X-ray Diffraction (XRD) Analysis

Dried silver nanoparticles from *O. latifolia* leaf extract were coated on an XRD grid. The corresponding spectra were recorded by using the XPERT-PRO PANalytical instrument, which operates at a voltage of 45 kV and a current of 30 mA with CuK α radiation source using Ni as a filter. All X-ray diffraction data were collected under the experimental conditions in the regular angular range. The crystalline size of silver nanoparticles was calculated from the width of the XRD peaks, using the Debye-Scherrer formula (Eq. 3).

Where D is the average crystalline domain size perpendicular to the reflecting planes, λ is the X-ray wavelength, β is the full width at half maximum, and θ is the diffraction angle.

FTIR Analysis

The characterisation of functional groups on the surface of AgNPs was performed by Fourier-transform infrared

$$\% \text{Inhibition} = \frac{\text{Control OD} - \text{Sample OD}}{\text{Control OD}} \times 100 \quad (\text{Eq. 2})$$

$$D = \frac{0.94\lambda}{\beta \cos \theta} \quad (\text{Eq. 3})$$

spectroscopy (FTIR) – SHIMADZU (Miracle 10), and the spectra were scanned in the 500-4000 cm^{-1} range at a resolution of 4 cm^{-1} .

***In Vitro* Anti-inflammatory Assay**

Protein Denaturation Assay

The reaction mixture (0.5 mL) was prepared by dissolving 0.4 mL of Bovine serum albumin (2 % aqueous solution), 0.05 mL of distilled water, and then the mixture was added to different concentrations (20, 40, 60, 80 and 100) of the sample. They were then incubated at 37 °C for 30 min and then heated at 57 °C for 10 min. After cooling, 2.5 mL of phosphate-buffered saline (pH 7.4) was added to each test tube. Ibuprofen was used as the standard drug, while the reaction mixture without the sample served as the negative control. All experiments were performed in triplicate, and the absorbance was measured at 600 nm

using a UV-spectrophotometer (20). This procedure was specifically designed to evaluate the capability of the plant extract to inhibit protein denaturation under thermal stress.

Results

Extractive Yield Percentage

In the present study, the fresh plant specimens (**Figure 1** and **2**) were sequentially extracted using solvents of increasing polarity (**Figure 3** and **4**). Extractive yield percentage represents the amount of active constituents extracted from the plant species, and it varied significantly ($p < 0.05$) among different solvents and plant parts, with values ranging from 1.63 to 13.83% in leaves and 1.04 to 20.65% in stems, respectively. However, among the plant parts assessed, the ethanolic extract of both the leaf and stem registered a high amount of extractive yield

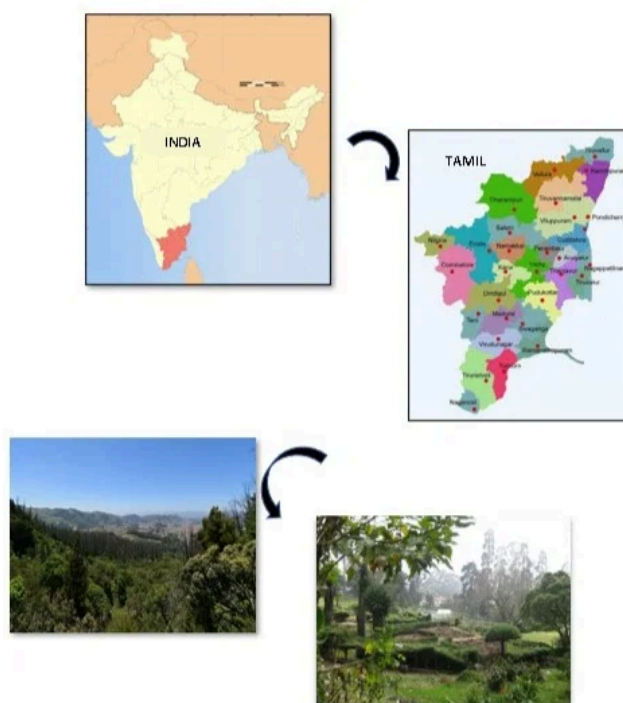


Figure 1. Map and field photographs of the sampling area: The sequence shows the study location starting from the national level (India), moving to the state level (Tamil Nadu), and finally the specific natural habitat in the Nilgiris where *Oxalis latifolia* samples were collected.



Figure 2. Habit of *Oxalis latifolia*.

percentage (13.83% & 20.65%). The enhanced extraction efficiency observed with the moderately polar ethanol is attributed to its ability to solubilise a broad spectrum of polar and semi-polar phytoconstituents, including phenolics and flavonoids.

Proximate composition analysis

Proximate composition is used for estimating substances such as total protein, carbohydrates, and crude lipids. This helps to analyse the total amount of macromolecular contents present in the plant sample, and these macromolecular constituents contribute to antioxidant mechanisms and can potentially act as stabilising or capping agents during the green synthesis of silver nanoparticles. (Table 1) depicts the total amount of protein, carbohydrate and crude lipid content of leaf and stem extracts of *O. latifolia*. Among the two extracts

analysed, the leaf extract evidenced a higher amount of protein, carbohydrate and crude lipid contents.

Phytochemical Screening

Preliminary Qualitative Phytochemical Analysis of Primary and Secondary Metabolites

Preliminary qualitative phytochemical screening was conducted to obtain an initial indication of major classes, including alkaloids, flavonoids, phenolics, glycosides, and carbohydrates (Table 2). Among the various solvent types examined, all the solvent extracts exhibited positive reactions with respect to colour-based assays, suggesting the probable presence of these phytoconstituents.

Quantitative Phytochemical Analysis of Secondary Metabolites

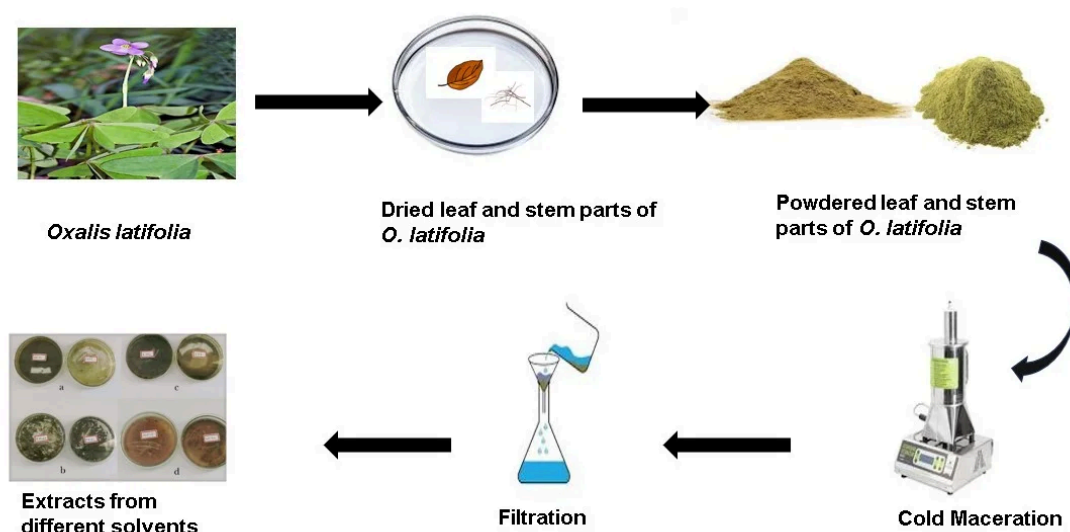


Figure 3. Extraction process of *Oxalis latifolia* using the cold maceration technique.

Table 1. Proximate compositional analysis of *O. latifolia* leaf and stem parts.

Sample	Plant part	Protein	Carbohydrate	Crude Lipid %
<i>Oxalis latifolia</i> Kunth.	Leaf	19.86 ± 2.61	58.61 ± 2.78	3.43
	Stem	11.24 ± 1.55	33.12 ± 1.83	1.04

Table 2. Preliminary qualitative phytochemical analysis of leaf and stem parts of *O. latifolia*.

Phytochemical test	Leaf				Stem			
	PE	EA	Eth	Aq	PE	EA	Eth	Aq
Alkaloid	+++	+++	+++	+++	++	++	+++	+++
Flavonoid	++	++	+++	++	+	+	++	++
Phenolics	++	+++	+++	++	++	++	+++	++
Glycosides	+	+	++	+	+	+	+	+
Carbohydrates	++	++	+++	+++	+++	+	+++	+++

Note: PE-Petroleum ether; EA-Ethyl acetate; Eth-Ethanol; Aq-Aqueous * +++ (Abundant), ++ (Moderate), + (Trace)

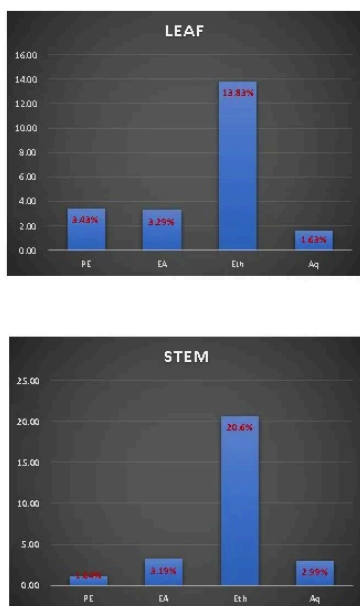


Figure 4. Extractive yield percentage for leaf and stem parts of *Oxalis latifolia*.

Phenolics are a significant class of bioactive compounds with a wide range of biological actions. Based on this, the Folin-Ciocalteu reagent was used to determine the phenolic content of *O. latifolia* leaf and stem part extracts (**Table 3**). The overall phenolic content for both the plant parts varied greatly, ranging from 5.58 to 79.32 mg GAE/g of extract. Among the samples evaluated, the ethanolic extracts of *O. latifolia* leaf and stem parts showed the highest total phenolic content, with 58.64 mg GAE/g and 79.32 mg GAE/g, respectively. In general, ethanol > water > petroleum ether > ethyl acetate was the order in which phenolics were most effectively extracted.

Total Tannins

Tannins are more prevalent and most likely to be found in all plant parts. Using recognised standard protocols, the tannin concentrations of different extracts of *O. latifolia*

leaf and stem parts were obtained and expressed as Gallic acid equivalents (**Table 3**). Both leaf and stem part extracts have tannin contents ranging from 2.01 to 69.33 mg GAE/g. The ethanolic extracts of the leaf and stem parts had higher tannin contents ranging between 52.82 mg GAE/g and 69.33 mg GAE/g, respectively. On the other hand, the leaf ethyl acetate fractions (3.88 mg GAE/g) and the stem petroleum ether fractions (2.01 mg GAE/g) had the lowest tannin concentration.

Total Flavonoid Content

Flavonoids are the most significant plant secondary metabolites distributed throughout the plant kingdom. In this study, the content of total flavonoids for leaf and stem parts of *O. latifolia* varied considerably among the plant parts and solvent systems examined (**Table 3**). The highest flavonoid content was observed in the ethanolic extracts of leaf and stem parts, having values ranging from 62.50 mg RE/g and 54.17 mg RE/g. However, the lowest flavonoid content was exhibited for the petroleum ether extracts of leaf (8.06 mg RE/g) and stem (4.72 mg RE/g).

Total Flavanol Content

The present investigation revealed notable variations in the total flavanol content of *O. latifolia* leaf and stem parts across the different solvent systems analysed (**Table 3**). The ethanolic extracts of the leaf and stem portions displayed the highest flavanol content, with values of 55.20 mg RE/g and 59.13 mg RE/g, respectively. However, the petroleum ether extracts of the leaf (13.32 mg RE/g) and stem (15.71 mg RE/g) exhibited the lowest flavanol content among the tested solvent systems.

Determination of *In Vitro* Antioxidant Activity

Free Radical Scavenging Ability Using DPPH* Assay

The ability of the plant samples to scavenge free radicals was assessed using the DPPH assay, a highly stable organic radical that exhibits a strong absorption band at 517 nm in visible spectroscopy (**Table 4**). All evaluated samples in this investigation were able to effectively interact with DPPH and convert its stable purple colour to yellow. In contrast to other solvent extracts, the ethanolic extracts of the leaf and stem exhibited comparatively

Table 3. Quantification of secondary metabolites for leaf and stem parts of *O. latifolia*.

Sample	Plant part	Extracts*	Total Phenol [#]	Free Phenol [#]	Total Tannins [#]	Total Flavonoid [¥]	Total Flavanol [¥]
<i>Oxalis latifolia</i> Kunth.	Leaf	PE	6.02 ± 0.10	1.31 ± 0.22	4.71 ± 0.15	8.06 ± 0.48	13.32 ± 2.63
		EA	5.15 ± 0.10	1.27 ± 0.08	3.88 ± 0.26	48.61 ± 3.47	18.10 ± 0.51
		Eth	58.64 ± 0.54	5.81 ± 0.42	52.82 ± 0.18	62.50 ± 4.11	55.20 ± 1.57
		Aq	15.53 ± 0.09	0.48 ± 0.03	5.05 ± 0.07	15.56 ± 1.53	38.44 ± 2.58
	Stem	PE	2.33 ± 0.01	0.32 ± 0.01	2.01 ± 0.02	4.72 ± 0.48	15.71 ± 0.78
		EA	5.58 ± 0.09	1.23 ± 0.04	4.75 ± 0.13	17.50 ± 2.50	32.80 ± 0.30
		Eth	79.32 ± 0.96	9.99 ± 0.46	69.33 ± 0.03	54.17 ± 3.63	59.13 ± 2.56
		Aq	10.14 ± 0.13	1.02 ± 0.04	9.14 ± 0.12	25.83 ± 2.50	44.43 ± 1.63

Note: PE-Petroleum ether; EA-Ethyl acetate; Eth-Ethanol; Aq-Aqueous *Values are mean±SD of three independent experiments. [#]Values were expressed as mg GAE/g extract; [¥]Values were expressed as mg RE/g extract

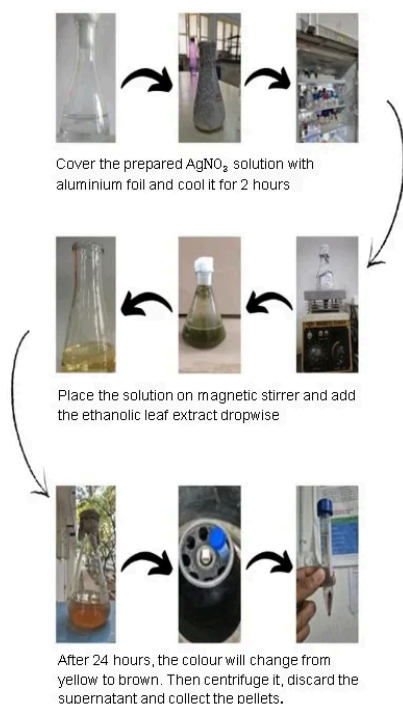


Figure 5. Green synthesis of silver nanoparticles using ethanolic leaf extract of *O. latifolia*.

lower IC₅₀ values (92.18 µg/mL and 101.22 µg/mL, respectively).

ABTS^{•+} Radical Scavenging Activity

The enhanced ABTS^{•+} radical decolourisation assessment was utilised to quantify the Trolox equivalent antioxidant capacity (TEAC). The ABTS^{•+} cation radical's decolourisation provides a clear indicator of the plant samples' antioxidant capacity. All extracts exhibited radical scavenging activity, though variations were observed across solvent systems (**Table 4**). Interestingly, petroleum ether extracts of leaf and stem exhibited comparatively higher TEAC values (2204.39 µmol TE/g extract for leaf and 1368.82 µmol TE/g extract for stem), despite showing lower phenolic content. This variation may be attributed to the presence of non-phenolic, lipophilic antioxidant constituents extracted in petroleum ether.

Phosphomolybdenum Assay

The total antioxidant capacity (TAC) of the plant sample can be measured using the phosphomolybdenum assay. The process depends on antioxidants found in the plant sample reducing molybdenum (VI) to molybdenum (V), which forms a compound comprising green phosphomolybdenum (V). Relatively higher antioxidant ability was noticed in the ethanolic extracts of the leaf and stem samples (28.48 µg/mL for leaf and 9.16 µg/mL), respectively (**Table 4**).

Green Synthesis of Silver Nanoparticles

The major advantage of using plant extracts for synthesising silver nanoparticles is that they are easily available, safe and nontoxic in most cases. The green synthesis of silver nanoparticles (AgNPs) using leaf extracts of *O. latifolia* was carried out in the present study. The colour was changed from pale yellow to dark brown within 24 h when 1 mM of silver nanoparticles were added to the leaf extracts. These attained the maximum intensity after 12 h with increased intensity during the period of incubation, which indicates the formation of green synthesis of silver nanoparticles (AgNPs) (**Figure 5**).

Characterisation of Silver Nanoparticles

Characterisation of silver nanoparticles was initially conducted using the UV-Visible spectrum, indicated by the appearance of the surface plasmon resonance peak. Morphological confirmation was further obtained through SEM imaging and X-ray diffraction analysis, which displayed distinct diffraction peaks corresponding to face-centred cubic silver. Elemental composition was further verified by EDS analysis, confirming the presence of silver as the major constituent.

UV-visible Spectroscopy Of Green-synthesised AgNPs from Leaf Extract of *O. latifolia*

The UV-Vis spectral analysis for the ethanolic leaf extract-mediated silver nanoparticles of *O. latifolia* indicates successful nanoparticle synthesis (**Figure 6**). The absorbance spectrum shows a distinct surface plasmon resonance (SPR) peak at approximately 405 nm, suggesting the formation of silver nanoparticles, as AgNPs typically exhibit an SPR band in the range of 400–450 nm. The optical density (OD) values further support this, with OD 405 reaching 0.760, the highest recorded in the visible

Table 4. *In vitro* antioxidant assays for leaf and stem parts of *O. latifolia*.

Sample	Plant part	Extracts	DPPH (IC ₅₀ in µg/mL)	ABTS ^{•+}	Phosphomolybdenum assay
<i>Oxalis latifolia</i> Kunth.	Leaf	PE	195.15 ± 0.01	2204.39 ± 10.17	17.15 ± 0.20
		EA	201.22 ± 0.22	1069.80 ± 8.47	13.70 ± 0.08
		Eth	92.18 ± 0.51	1475.13 ± 5.23	28.48 ± 0.08
		Aq	122.37 ± 0.07	1984.63 ± 2.38	19.53 ± 0.08
	Stem	PE	201.59 ± 0.22	1368.82 ± 10.41	3.45 ± 0.20
		EA	197.65 ± 0.64	1269.15 ± 7.10	5.73 ± 0.27
		Eth	101.22 ± 0.14	1103.03 ± 7.16	9.16 ± 0.25
		Aq	130.55 ± 0.28	1250.87 ± 4.98	5.06 ± 0.16

Note: Values are mean ± SD of three independent experiments.

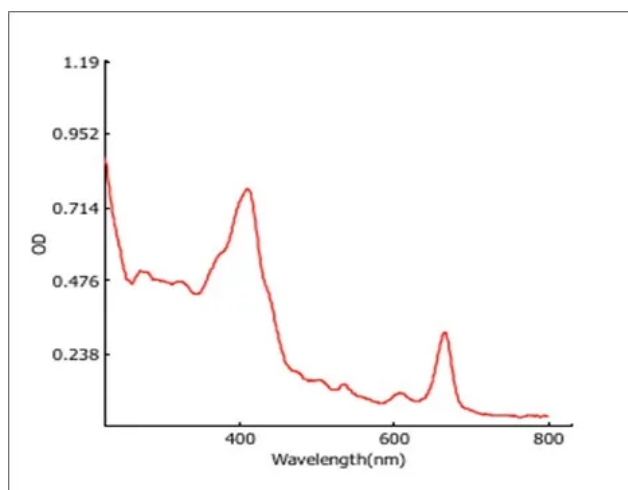


Figure 6. UV-Visible spectroscopy analysis of green-synthesised silver nanoparticles from the ethanolic leaf extract of *O. latifolia*.

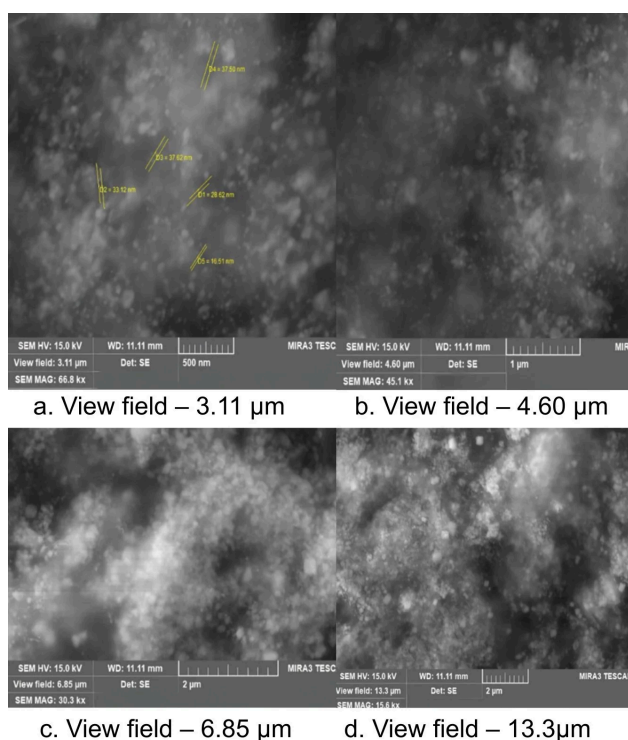


Figure 7. SEM analysis of green-synthesised silver nanoparticles from the ethanolic leaf extract of *O. latifolia*.

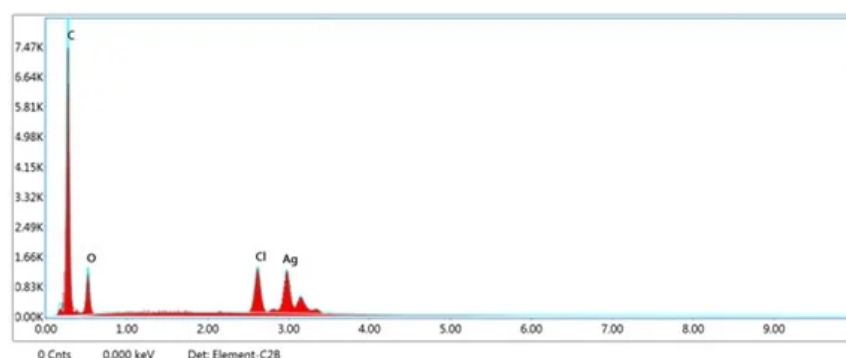


Figure 8. EDX analysis of green-synthesised silver nanoparticles from the ethanolic leaf extract of *O. latifolia*.

range, reinforcing nanoparticle formation. Additional absorption peaks were observed at 220 nm and 250 nm (with OD values of 0.928 and 0.508, respectively), which may correspond to the presence of biomolecules such as flavonoids, proteins, or phenolic compounds involved in the reduction and stabilisation of AgNPs. The decreasing absorbance beyond 500 nm and towards 800 nm (OD 600 = 0.102, OD 800 = 0.036) indicates the absence of significant aggregation or large particle formation. The path length of 0.651 mm and a dilution factor of 1.000 confirm that the sample was analysed in its original concentration without modifications. Overall, these findings confirm the successful biosynthesis of AgNPs with strong SPR absorption and potential bioactive molecule interactions aiding in stabilisation.

Scanning Electron Microscopy of Green-synthesised AgNPs from the Leaf Extract of *O. latifolia*

The SEM-EDX analysis for the silver nanoparticles (AgNPs) synthesised from the ethanolic leaf extract of *O. latifolia* confirms a substantial presence of silver, with weight percentages of 19.53% and 18.85% validating the efficiency of the green synthesis process (**Figure 7 & 8**). Although the atomic percentages of silver were lower (2.96% and 2.82%, respectively), this is expected due to the high atomic weight of carbon. In addition to silver, the EDX spectra reveal the presence of carbon (57.32% and 58.14% by weight) and oxygen (15.15% and 15.26% by weight), suggesting the involvement of phytochemicals in the reduction, capping, and stabilisation of the nanoparticles. These biomolecules are likely to originate from flavonoids, polyphenols, and other secondary metabolites in the plant extract, which serve as both reducing and stabilising agents. Chlorine (8.00% and 7.75% by weight) was also detected, possibly due to residual plant compounds or precursor salts used in the synthesis. Overall, these results affirm the potential of this plant extract as an efficient bio-reductant for eco-friendly nanoparticle synthesis, providing a promising avenue for biomedical and nanotechnological applications.

X-ray Diffraction Analysis on Green-synthesised AgNPs from the Leaf Extract of *O. latifolia*

The X-ray diffraction (XRD) analysis for the synthesised silver nanoparticles (AgNPs) provides insight into their crystalline nature, phase purity, and structural

characteristics (**Figure 9**). characteristic peaks at 38.12° and 43.70° are characteristic of the (111) and (200) planes of face-centred cubic (FCC) silver, validating the successful formation of AgNPs (**Table 5**). The strong peaks at 23.34° and moderate peaks at 26.88° and 30.25° may be due to the biomolecules from the plant extract acting as capping agents. Peak broadening and FWHM values indicate nanocrystalline particle size with the (111) plane showing preferential orientation. The lack of significant impurity

peaks corresponding to silver oxides (Ag_2O) or silver chloride (AgCl) suggests that the synthesised AgNPs exhibit high purity. Overall, the XRD analysis further confirms the formation of FCC-structured crystalline silver nanoparticles.

Fourier Transform Infrared Microscopy of Green-synthesised AgNPs from the Leaf Extract of *O. latifolia*

The Fourier Transform Infrared (FTIR) spectrum of the

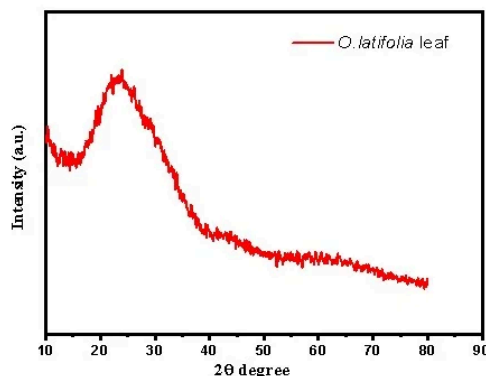


Figure 9. XRD analysis of green-synthesised silver nanoparticles from the ethanolic leaf extract of *O. latifolia*.

Table 5. XRD analysis of green-synthesised silver nanoparticles.

No.	Pos. [2θ]	d-spacing [Å]	FWHM [2θ]	Area [cts* 2θ]	Backgr. [cts]	Height [cts]	Crys. Size	Avg. size (nm)
1	23.34	3.81	0.47	52.12	293	109.28	16.31	
2	26.88	3.31	1.36	74.78	266	82.31	5.66	
3	30.25	2.95	0.34	17.87	227	76.92	22.01	
4	38.12	2.36	0.09	0.3	126	4.99	83.42	
5	43.70	2.07	0.09	0.99	112	11.04	81.92	56.68
6	53.97	1.69	0.09	0.61	89	6.79	78.65	
7	61.73	1.50	0.09	0.09	87	1	75.76	
8	62.23	1.49	0.09	0.09	87	1	75.56	
9	73.36	1.29	0.09	0.09	67	1	70.78	

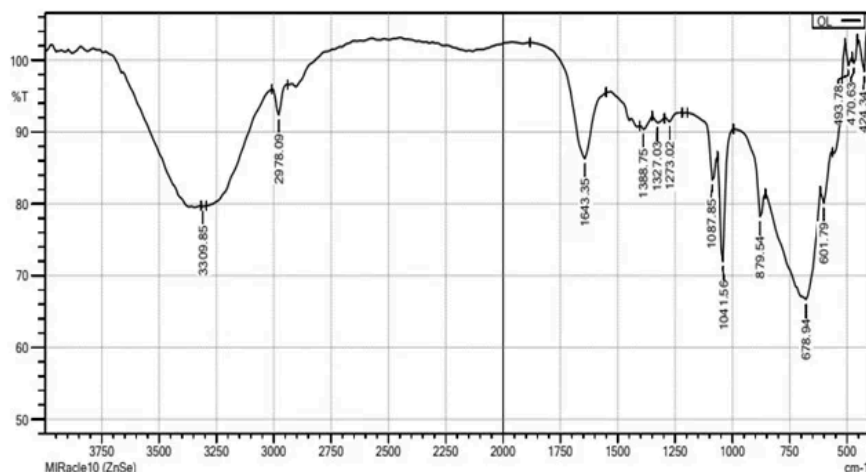


Figure 10. FTIR analysis of green-synthesised silver nanoparticles from the ethanolic leaf extract of *O. latifolia*.

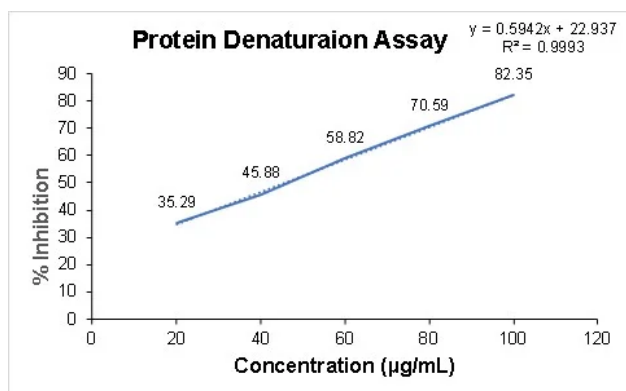


Figure 11. Anti-inflammatory activity of green-synthesised silver nanoparticles from *O. latifolia* evaluated using the protein denaturation assay.

synthesised silver nanoparticles (AgNPs) reveals the presence of various functional groups responsible for the reduction, stabilisation, and capping of the nanoparticles (Figure 10). The broad absorption band observed at 3309.85 cm^{-1} corresponds to the O–H stretching vibration of hydroxyl groups, indicating the presence of phenolic or alcoholic compounds. This suggests the involvement of plant-derived polyphenols in the reduction and stabilisation of silver ions during nanoparticle synthesis. The peak at 2978.09 cm^{-1} corresponds to C–H stretching vibrations of alkanes, while the peak at 1643.35 cm^{-1} is assigned to C=O stretching of carbonyl groups, which could be attributed to carboxylic acids, flavonoids, or ketones present in the plant extract. The presence of peaks at 1388.75 cm^{-1} , 1327.03 cm^{-1} , and 1273.02 cm^{-1} further supports the existence of C–O stretching vibrations, indicative of phenolic, ether, or ester functional groups. The peaks at 1087.85 cm^{-1} and 1041.56 cm^{-1} correspond to C–O–C and C–O stretching vibrations, which further confirm the involvement of polysaccharides or flavonoids in the capping process. The strong absorption peak at 879.54 cm^{-1} suggests aromatic C–H bending, indicating the presence of aromatic compounds that could contribute to the stability of AgNPs. Additionally, peaks at 678.94 cm^{-1} , 601.79 cm^{-1} , 493.78 cm^{-1} , 470.63 cm^{-1} , and 424.34 cm^{-1} in the lower frequency region correspond to metal-oxygen bonds, particularly Ag–O interactions, confirming the successful binding of biomolecules onto the surface of silver nanoparticles.

Determination of Anti-inflammatory Effect by Protein Denaturation Assay

The protein denaturation assay results indicate that the silver nanoparticles derived from the ethanolic extract of *O. latifolia* leaves exhibited concentration-dependent anti-inflammatory activity (Figure 11), with inhibition increasing from 35.29% at $20\text{ }\mu\text{g/mL}$ to a maximum of 82.35% at $100\text{ }\mu\text{g/mL}$. This trend suggests that nanoparticles effectively stabilise proteins against heat-induced denaturation, a key mechanism in inflammatory processes.

Discussion

The phytochemical and antioxidant profiling of *O. latifolia* reveals significant insights into its potential medicinal benefits, and its comparative efficacy among species

within the genus *O. latifolia* stands out due to its high flavonoid and phenolic acid content, which correlates with substantial antioxidant activity. Its remarkable free radical scavenging capacities, as demonstrated through various assays, including DPPH and ABTS radical scavenging tests (21). These findings are compatible with the antioxidant profiles observed in other *Oxalis* species.

For instance, *O. corniculata* has shown considerable antioxidant activity in the DPPH radical scavenging assay, which is comparable to that of *O. latifolia* (22). Likewise, *O. acetosella* exhibits notable antioxidant activity through its phenolic extracts, which provide a robust defence against oxidative stress. These similarities suggest that a common mechanism of action may underlie the antioxidant effects across these species.

Comparative studies of the *Oxalis* species highlight that *O. latifolia* shares similar medicinal potential with its relatives. Research on *O. corniculata* has demonstrated its anti-inflammatory and anti-diabetic properties, which are at least partially attributed to its antioxidant activity (23). Analogously, *O. acetosella* has been shown to alleviate conditions related to oxidative stress, further indicating a potential common pathway for these beneficial effects (24).

A detailed phytochemical analysis of *O. triangularis* discloses a diverse array of compounds, including flavonoids, glycosides, alkaloids, carbohydrates, saponins, and steroids, while tannins, proteins, and resins are absent (21). Similarly, preliminary qualitative evaluation of leaf extracts of *Biophytum sensitivum*, another genus in the family Oxalidaceae, has been identified to have cardiac glycosides, flavonoids, tannins, sterols, and carbohydrates (25). These findings support the phytochemical profile observed in *O. latifolia*, emphasising its rich content of flavonoids and phenolic compounds.

Quantitative analysis of *O. triangularis* revealed substantial content of total phenolics and flavonoid content (26). While the total phenolic content in *O. latifolia* is relatively lower compared to *O. triangularis*, its flavonoid content is notably higher. The difference in flavonoid levels might contribute to the observed variation in antioxidant efficacy.

Furthermore, the antioxidant activity of *O. triangularis*, particularly in its petroleum ether extract, is evidenced by its effective DPPH scavenging activity with an IC_{50} value of $125.429\text{ }\mu\text{g/mL}$ (26). However, *O. latifolia* demonstrates a significantly higher IC_{50} value for its ethanolic extracts from leaf and stem parts, indicating good DPPH scavenging action. This enhanced antioxidant activity in *O. latifolia* suggests that its extracts may be more potent in neutralising free radicals compared to those of *O. triangularis*. Thus, the comparative analysis of *O. latifolia* and related species underscores its promising antioxidant efficacy and medicinal potential. The higher flavonoid content and promising DPPH scavenging ability of *O. latifolia* suggest that it could be a valuable candidate for further pharmacological studies and therapeutic applications.

The green synthesis of silver nanoparticles (AgNPs) using *O. latifolia* presents a sustainable and eco-friendly approach to nanotechnology. Biosynthesis of nanoparticles is a kind of bottom-up approach. The major advantage of using plant extracts for silver nanoparticle synthesis is that they are easily available, safe, and

nontoxic in most cases (27). The successful green synthesis of silver nanoparticles (AgNPs) using the ethanolic leaf extract of *O. latifolia* evidenced a notable colour change from pale yellow to dark brown within 24 h and a distinct surface plasmon resonance (SPR) absorbance at 405 nm, consistent with the typical SPR band in the 400–450 nm range. This report is in good agreement with the previous reports on *O. corniculata*, which yielded a characteristic SPR peak (445 nm) and similar visual colour change (28). The additional absorption peaks (220–250 nm) observed at the UV-visible spectroscopy of green-synthesised AgNPs reflect the presence of phytoconstituents such as flavonoids, phenolics, and proteins acting as reducing and capping agents. This aligns with the mechanism of biogenic synthesis of plant-derived secondary metabolites that donate electrons (reducing Ag^+ to Ag^0) and thereafter stabilise the nanoparticles to prevent aggregation (29). Morphological and compositional analyses further strengthen the case for successful green synthesis. The SEM-EDX results show substantial silver content along with significant carbon and oxygen percentages, which strongly suggests that organic biomolecules from the plant extract remain associated with the AgNP surface, plausibly providing stabilisation via capping. Such residual organic moieties are commonly observed in plant-mediated AgNPs (30). The XRD data indicate peaks at 38.12° and 43.70° corresponding to the (111) and (200) planes of face-centred cubic (FCC) silver, which affirms the crystalline nature and phase purity of the synthesised AgNPs. Similar observations have been made in other biosynthesised AgNPs (31). The average crystalline size of the synthesised AgNPs was estimated based on the XRD peak broadening, which represents crystalline structure rather than complete particle size. SEM analysis was primarily employed to examine particle morphology and surface characteristics; detailed size distribution analysis was not performed.

The FTIR spectrum of *O. latifolia*-derived AgNPs reveals prominent O-H stretching (3309 cm^{-1}), C-H stretching (2980 cm^{-1}), carbonyl/amide bands (1643 cm^{-1}), and C-O/C-O-C vibrations ($1388\text{--}1040\text{ cm}^{-1}$), indicating the presence of polyphenols, flavonoids, proteins, and polysaccharides, which act collectively as reducing and capping agents. This pattern is similarly observed in other plant species, like *Sida schimperiana* and *Oxalis griffithii* (32, 33). *O. latifolia* AgNPs showed strong dose-dependent inhibition of protein denaturation, indicating significant anti-inflammatory activity comparable to other plant-derived AgNPs, including the reports from *Zingiber officinale* and *Ocimum gratissimum*, which achieved up to (~ 78%) protection against albumin denaturation under identical assay conditions (34). These similarities that are observed in different genera underscore that the anti-inflammatory effects of plant-derived AgNPs primarily arise from the phytochemical-rich capping layers, especially of phenolics and flavonoids, which enhance nanoparticle stability and protein-protective interactions, hence supporting the strong anti-inflammatory activity observed in *O. latifolia* AgNPs.

Conclusion

In the Indian traditional system of medicine, the use of the *Oxalis* genus is well evidenced from earlier literature, as the plants have been extensively used for the treatment of

jaundice, mouth ulcers, abdominal pain, and so on. The present study provides fundamental scientific validation of *O. latifolia* through phytochemical screening, *in vitro* antioxidant evaluation and biosynthesis of silver nanoparticles (AgNPs). Qualitative and quantitative analyses confirmed the presence of major bioactive constituents, including phenolic compounds, flavonoids, tannins, and flavanols, particularly in the ethanolic extracts of leaf and stem. The *in vitro* antioxidant assays demonstrated concentration-dependent free radical scavenging activity, indicating the potential of the extracts as natural antioxidant sources under experimental conditions. Furthermore, the successful synthesis of AgNPs from the ethanolic extract was confirmed through physicochemical characterisation, and the nanoparticles exhibited measurable anti-inflammatory activity. However, this study was limited to *in vitro* assays; further investigations, including compound isolation and *in vivo* validation, are required.

Abbreviations

PVPP = Polyvinylpyrrolidone; DPPH = 2, 2-diphenyl-1-picrylhydrazyl; $\text{ABTS}^{+\cdot}$ = 2, 2' - azino-bis (3-ethylbenzothiazoline-6-sulfonic acid); GAE = Gallic Acid Equivalent; RE = Rutin Equivalent; SPR = Surface Plasmon Resonance.

Declaration

Author Information

Malavika J

PG and Research Department of Botany, Kongunadu Arts and Science College, GN Mills, Coimbatore, Tamil Nadu - 641 029, India.

Contribution: Conceptualization, Data Curation, Investigation, Methodology, Writing - Original Draft.

Athira P

PG and Research Department of Botany, Kongunadu Arts and Science College, GN Mills, Coimbatore, Tamil Nadu - 641 029, India.

Contribution: Conceptualization, Data Curation, Methodology.

Gayathri G

PG and Research Department of Botany, Kongunadu Arts and Science College, GN Mills, Coimbatore, Tamil Nadu - 641 029, India.

Contribution: Investigation, Methodology.

Slowmo M

PG and Research Department of Botany, Kongunadu Arts and Science College, GN Mills, Coimbatore, Tamil Nadu - 641 029, India.

Contribution: Investigation, Methodology.

Thenmozhi Krishnasamy

*Corresponding author

PG and Research Department of Botany, Kongunadu Arts and Science College, GN Mills, Coimbatore, Tamil Nadu - 641 029, India.

Contribution: Conceptualization, Formal analysis, Project administration, Supervision, Validation, Writing-Review &

Editing.

Acknowledgment

The authors would like to express their profound gratitude towards the Department of Botany, Kongunadu Arts and Science College, Coimbatore, for their constant support and assistance in finishing this work.

Conflict of Interest

The authors declare no conflicting interest.

Data Availability

Upon request

Ethics Statement

Not applicable

Funding Information

The author(s) declare that no financial support was received for the research, authorship, and/or publication of this article.

References

- Cragg GM, Newman DJ. Natural products: A continuing source of novel drug leads. *Biochimica et Biophysica Acta (BBA) - General Subjects*. 2013;1830(6):3670-3695. doi: <https://doi.org/10.1016/j.bbagen.2013.02.008>
- Alencar ERD, Faroni LRD, Peternelli LA, Silva MTCD, Costa AR. Influence of soybean storage conditions on crude oil quality. *Rev. bras. eng. agríc. ambient*. 2010;14(3):303-308. doi: <https://doi.org/10.1590/s1415-43662010000300010>
- Godswill AG, Somtochukwu IV, Ikechukwu AO, Kate EC. Health Benefits of Micronutrients (Vitamins and Minerals) and their Associated Deficiency Diseases: A Systematic Review. *Ijff*. 2020;3(1):1-32. doi: <https://doi.org/10.47604/ijff.1024>
- Sampaio BL, Edrada-Ebel R, Da Costa FB. Effect of the environment on the secondary metabolic profile of *Tithonia diversifolia*: a model for environmental metabolomics of plants. *Sci Rep*. 2016;6(1). doi: <https://doi.org/10.1038/srep29265>
- Oberlander KC, Dreyer LL, Roets F. Oxalidaceae. *Bothalia*. 2010;40(2):177-178. doi: <https://doi.org/10.4102/abc.v40i2.211>
- Junejo JA. Antidiabetic and Antioxidant Activity of Hydro-Alcoholic Extract of *Oxalis Debilis* Kunth Leave in Experimental Rats. *Biosci. Biotech. Res. Comm*. 2020;13(2):860-867. doi: <https://doi.org/10.21786/bbrc/13.2/71>
- Chawdhry MA, Sagar GR. Control of *Oxalis latifolia* H.B.K. and *O. pes-caprae* L. by defoliation. *Weed Research*. 1974;14(5):293-299. doi: <https://doi.org/10.1111/j.1365-3180.1974.tb01064.x>
- Gitari JK. Antibacterial, antifungal, anti-inflammatory, and antiscorbutic properties of *Oxalis* species. *Int. J. Phytomedicine*. 1986;4(2): 101-107.
- Harborne JB. *Organic Acids, Lipids and Related Compounds*. Dordrecht: Springer Netherlands; 1984. doi: https://doi.org/10.1007/978-94-009-5570-7_4
- Chandran R, Thangaraj P, Shanmugam S, Thankarajan S, Karuppusamy A. Antioxidant and anti-inflammatory potential of *monochoria vaginalis* (burm. f.) c. presl.: a wild edible plant. *Journal of Food Biochemistry*. 2011;36(4):421-431. doi: <https://doi.org/10.1111/j.1745-4514.2011.00560.x>
- Richardson PM, Harborne JB. *Phytochemical Methods: A Guide to Modern Techniques of Plant Analysis*. Second Edition. *Brittonia*. 1990;42(2):115. doi: <https://doi.org/10.2307/2807624>
- Makkar HPS. *Quantification of Tannins in Tree and Shrub Foliage*. Dordrecht: Springer Netherlands; 2003. doi: <https://doi.org/10.1007/978-94-017-0273-7>
- Zhishen J, Mengcheng T, Jianming W. The determination of flavonoid contents in mulberry and their scavenging effects on superoxide radicals. *Food Chemistry*. 1999;64(4):555-559. doi: [https://doi.org/10.1016/s0308-8146\(98\)00102-2](https://doi.org/10.1016/s0308-8146(98)00102-2)
- Miliauskas G, Venskutonis P, van Beek T. Screening of radical scavenging activity of some medicinal and aromatic plant extracts. *Food Chemistry*. 2004;85(2):231-237. doi: <https://doi.org/10.1016/j.foodchem.2003.05.007>
- Blois MS. Antioxidant Determinations by the Use of a Stable Free Radical. *Nature*. 1958;181(4617):1199-1200. doi: <https://doi.org/10.1038/1811199a0>
- Re R, Pellegrini N, Proteggente A, Pannala A, Yang M, Rice-Evans C. Antioxidant activity applying an improved ABTS radical cation decolorization assay. *Free Radical Biology and Medicine*. 1999;26(9-10):1231-1237. doi: [https://doi.org/10.1016/s0891-5849\(98\)00315-3](https://doi.org/10.1016/s0891-5849(98)00315-3)
- Prieto P, Pineda M, Aguilar M. Spectrophotometric Quantitation of Antioxidant Capacity through the Formation of a Phosphomolybdenum Complex: Specific Application to the Determination of Vitamin E. *Analytical Biochemistry*. 1999;269(2):337-341. doi: <https://doi.org/10.1006/abio.1999.4019>
- Oves M, Aslam M, Rauf MA, Qayyum S, Qari HA, Khan MS, et al. Antimicrobial and anticancer activities of silver nanoparticles synthesized from the root hair extract of *Phoenix dactylifera*. *Materials Science and Engineering: C*. 2018;89:429-443. doi: <https://doi.org/10.1016/j.msec.2018.03.035>
- Iravani S. Green synthesis of metal nanoparticles using plants. *Green Chem*. 2011;13(10):2638. doi: <https://doi.org/10.1039/c1gc15386b>
- Bhat KI, Revanasiddappa BC, Kumar MV, Felicity B, Kumari R, Kumar A. Synthesis and *In-Vitro* Anti-Inflammatory Activity of New Pyrazoline Derivatives. *Rese. Jour. of Pharm. and Technol*. 2018;11(9):3969. doi: <https://doi.org/10.5958/0974-360x.2018.00729.1>

21. Krishnan RG, Muruges S. Antioxidant, Cytotoxic and larvicidal Potential in *Oxalis latifolia* Kunth. Methanolic Leaf Extract. *Jpri.* 2021;33(46A):269-275. doi: <https://doi.org/10.9734/jpri/2021/v33i46a32866>
22. Pandey K, Pokhrel S. Phytochemical Screening and Biological Activities of *Oxalis corniculata* Leaves of Sindhupalchowk District, Nepal. *Bibechana.* 2022;19(1-2):27-33. doi: <https://doi.org/10.3126/bibechana.v19i1-2.46094>
23. Kalauni SK, Mahato SK, Khanal LN. Phytochemical Studies and Toxicity Evaluation of Selected Medicinal Plants from Sarlahi District, Nepal. *J.PI.Reso.* 2023;21(1):21-31. doi: <https://doi.org/10.3126/bdpr.v21i1.57199>
24. Subramanian A, Suganya VN, Venkateswaran V. Evaluation of antihyperglycemic effect of *Oxalis latifolia* Kunth in streptozotocin-induced diabetic rats. *Indo Am. J. Pharm. Res.* 2019;9: 494-497.
25. Kala S. Phytochemical and Antimicrobial Analysis of Callus Extracts of *Biophytum sensitivum* (Linn) DC. *Bmrj.* 2014;4(8):869-884. doi: <https://doi.org/10.9734/bmrj/2014/7270>
26. Panda A, Chinmay P, Anath D. Phytochemical and cytogenetic studies of medicinally important *Oxalis* species occurring in India: A critical review. *Plant Sci Res.* 2017; 39 (1&2): 47-55.
27. Shahzadi S, Fatima S, ul ain Q, Shafiq Z, Janjua MRSA. A review on green synthesis of silver nanoparticles (SNPs) using plant extracts: a multifaceted approach in photocatalysis, environmental remediation, and biomedicine. *RSC Adv.* 2025;15(5):3858-3903. doi: <https://doi.org/10.1039/d4ra07519f>
28. Singh B, Kumar D, Soni M, Sinha J, Saroha P, Sharma K, et al. Larvicidal and anti-bacterial efficacy of silver nanoparticles derived from *Oxalis corniculata*. *Biosci Nanotechnol.* 2025;1(1). doi: <https://doi.org/10.1186/s44331-025-00002-6>
29. Ahmed RH, Mustafa DE. Green synthesis of silver nanoparticles mediated by traditionally used medicinal plants in Sudan. *Int Nano Lett.* 2019;10(1):1-14. doi: <https://doi.org/10.1007/s40089-019-00291-9>
30. Alsareii SA, Manaa Alamri A, AlAsmari MY, Bawahab MA, Mahnashi MH, Shaikh IA, et al. Synthesis and Characterization of Silver Nanoparticles from *Rhizophora apiculata* and Studies on Their Wound Healing, Antioxidant, Anti-Inflammatory, and Cytotoxic Activity. *Molecules.* 2022;27(19):6306. doi: <https://doi.org/10.3390/molecules27196306>
31. Akhter MS, Rahman MA, Ripon RK, Mubarak M, Akter M, Mahbub S, et al. RETRACTED: A systematic review on green synthesis of silver nanoparticles using plants extract and their bio-medical applications. *Heliyon.* 2024;10(11):e29766. doi: <https://doi.org/10.1016/j.heliyon.2024.e29766>
32. Moges W, Misskire Y. Green synthesis, characterization and antibacterial activities of silver nanoparticles using *Sida schimperiana* Hochst. ex A. Rich (Chifrig) leaves extract. *Discov Mater.* 2025;5(1). doi: <https://doi.org/10.1007/s43939-025-00221-x>
33. Singla S, Jana A, Thakur R, Kumari C, Goyal S, Pradhan J. Green synthesis of silver nanoparticles using *Oxalis griffithii* extract and assessing their antimicrobial activity. *OpenNano.* 2022;7:100047. doi: <https://doi.org/10.1016/j.onano.2022.100047>
34. Anandachockalingam A, Shanmugam R, Ryntathieng I, Dharmalingam Jothinathan MK. Green Synthesis of Silver Nanoparticles Using *Zingiber officinale* and *Ocimum gratissimum* Formulation for Its Anti-inflammatory and Antidiabetic Activity: An In Vitro Study. *Cureus.* 2024;16(4):e58098. doi: <https://doi.org/10.7759/cureus.58098>

Additional Information

How to Cite

APA 7th Edition: J, M., P, A., G, G., M, S. & Krishnasamy, T. (2026). Therapeutic Potential of *Oxalis latifolia*: Phytochemical Profiling and Green Synthesis of Functional Nanoparticles. *Sciences of Phytochemistry*, 5(1), 122-134. <https://doi.org/10.58920/sciphy0501522>

Vancouver: J M, P A, G G, M S, Krishnasamy T. Therapeutic Potential of *Oxalis latifolia*: Phytochemical Profiling and Green Synthesis of Functional Nanoparticles. *Sciences of Phytochemistry.* 2026;5(1):122-134. <https://doi.org/10.58920/sciphy0501522>

Harvard: J, M., P, A., G, G., M, S. & Krishnasamy, T. (2026) 'Therapeutic Potential of *Oxalis latifolia*: Phytochemical Profiling and Green Synthesis of Functional Nanoparticles', *Sciences of Phytochemistry*, 5(1), pp. 122-134. doi: 10.58920/sciphy0501522

Publisher Note

All claims expressed in this article are solely those of the authors and do not necessarily reflect the views of the publisher, the editors, or the reviewers. Any product that may be evaluated in this article, or claim made by its manufacturer, is not guaranteed or endorsed by the publisher. The publisher remains neutral with regard to jurisdictional claims in published maps and institutional affiliations.

Open Access

This article is licensed under a Creative Commons Attribution 4.0 International License. You may share and adapt the material with proper credit to the original author(s) and source, include a link to the license, and indicate if changes were made.